Laser Chem., Vol. 15, pp. 93–111
Reprints available directly from the Publisher
Photocopying permitted by license only

PHOTODISSOCIATION MECHANISMS OF BENZENE CLUSTER IONS ON THE EXCITATION WITH $h\nu$ = 0.5–3.0 eV

KAZUHIKO OHASHI, YASUHIRO NAKAI and NOBUYUKI NISHI

Department of Chemistry, Faculty of Science, Kyushu University, Hakozaki, Fukuoka 812, Japan

(Received 16 April, 1994)

The photodissociation of mass-selected benzene cluster ions, $(C_6H_6)_n^+$ (n = 2–8), is studied to elucidate the dynamics of dissociation and the mechanism of fragmentation. For $(C_6H_6)_2^+$, the average translational energy and the angular distributions of the photofragments are measured as a function of photon energy ($h\nu$). The photoexcitation to an upper bound state with $h\nu$ = 2.81 eV results in statistical energy disposal. Regardless of the excitation to a dissociative state with $h\nu$ = 1.17–1.62 eV, only a small fraction (at most 10%) of the available energy is partitioned into the translation. For $(C_6H_6)_n^+$ with n = 5–8, the average number of neutral molecules ejected following photoexcitation increases linearly with increasing $h\nu$ until $(C_6H_6)_2^+$ is reached as the product. The result suggests that the photofragmentation proceeds via the sequential evaporation of neutral monomers rather than the direct ejection of a neutral cluster.

KEY WORDS: photodissociation, dynamics, benzene, cluster ion, energy partitioning, unimolecular decay

1. INTRODUCTION

The photodissociation of size-selected cluster ions has been one of the most useful techniques for studying the property of photoexcited cluster ions as a function of cluster size.[1,2] Photodissociation spectroscopy utilizes the dissociation process as a means to detect photoabsorption. Several ionic complexes and clusters have been probed by this method.[3] Information has been provided on the geometrical and electronic structures and on the interaction between a chromophoric subunit and its environment.

The dynamics of photodissociation has also received much attention as another aspect of the photophysical properties of cluster ions. The rate of energy flow and the partitioning of the energy among the available modes have been examined for small cluster ions.[1] Photodissociation dynamics of the dimer ions such as $(NO)_2^+$, $(N_2)_2^+$ and $(CO_2)_2^+$ in the visible region was investigated by Bowers and co-workers.[4–6] The fraction of excess energy partitioned into relative translational energy was found to increase linearly with increasing photon energy. The product angular distributions

were well fitted with a simple expression. The derived anisotropy parameter was characteristic of the dissociation occurring on a repulsive surface. The photodissociation of $(C_6H_6)_2^+$ in the visible region was investigated by the same group.[7] At a photon energy of 2.71 eV, the translational energy distribution was found to be characteristic of statistical energy disposal. Thus a bound excited state was considered to be involved in the photodissociation. The previous spectroscopic studies by our group revealed that an intense absorption band of $(C_6H_6)_2^+$ in near-infrared region is due to a bound-free transition,[8–10] which corresponds to that of $(NO)_2^+$, $(N_2)_2^+$ and $(CO_2)_2^+$ observed in the visible region. One can expect the photophysical properties of $(C_6H_6)_2^+$ to be distinct from those of the dimer ions of the smaller molecules, because the density of states at a given total energy rises with the number of modes and, thus, the number of atoms.

The photodissociation studies of cluster ions of larger sizes can offer insights into the energetics of the cluster ions and the unimolecular decay dynamics of the energized clusters. About the decay mechanism, a question has been raised whether the fragmentation is due to evaporation of monomers or resulting from fission process. The photon-energy dependence of the average number of atoms or molecules ejected has given information on the type of fragmentation process. The fragmentation into a smaller cluster ion and a neutral cluster (namely, fission) was reported to be favourable for cluster ions of main-group elements (C, Si, Ge, Sb, Te, Bi and so forth).[11–15] This fission process is supported by the fact that the photofragmentation pattern is independent of the photon energy. On the other hand, the average number of the atoms lost in the photofragmentation of K_n^+ was found to be proportional to the photon energy.[16] Such a behavior was also observed in the photofragmentation of $(CO_2)_n^+$, $(CO_2)_n^-$ and Ar_n^+ by Lineberger and co-workers,[17–19] although the experiments were performed at a limited number of photoexcitation wavelengths. They concluded that the photofragmentation processes proceed via the ejection (evaporation)[20,21] of neutral monomers rather than the ejection of a neutral cluster. Recently, Beck and Hecht studied the photofragmentation of $(C_6H_6)_n^+$ with n = 7–15 in the 695–900-nm wavelength region.[22] They observed a smooth change in the size of the dominant fragment ion from n–3 to n–4 as the photon energy was increased continuously, suggesting the operation of the evaporative process.

In this article we describe the results on the photophysical properties of $(C_6H_6)_n^+$ with n = 2–8. A mass-selected ion beam of $(C_6H_6)_n^+$ is photodissociated by a laser beam with a crossed beam configuration. The major thrust of the present work is the wide range of the photon energies employed ($h\nu$ = 0.5–3.0 eV). The mass spectra of the fragment ions are recorded as functions of initial cluster size and photon energy. The time-of-flight (TOF) spectra of the neutral fragments are also measured to obtain quantitative information on the released translational energy and on the angular distributions. For $(C_6H_6)_2^+$, the experimental energy partitioning is compared with a calculated one according to the statistical theory in order to reveal dissociation mechanisms. For $(C_6H_6)_n^+$ with n = 3–8, the average number of ejected molecules is determined from the ratios of the observed fragment ion intensities. The photon-energy dependence of the number allows us to discuss photofragmentation mechanisms.

2. EXPERIMENTAL

Figure 1 depicts a schematic drawing of the experimental apparatus which combines a reflectron time-of-flight mass spectrometer (Jordan Co. Angular Reflectron) with a supersonic beam source for generating neutral clusters.[8,23] The $(C_6H_6)_n^+$ ions were produced by resonance-enhanced 2-photon ionization of the neutral clusters with the frequency-doubled output (210 nm) from a pulsed dye laser (Lumonics HyperDYE-300) pumped with an excimer laser (Lumonics HyperEX-400). The parent ions were then extracted along the Z axis with a typical birth potential of U_0 = 1450 ± 10 V. After traveling through a flight length of 0.36 m for mass selection, the ions were irradiated by a pulsed dissociation laser ($h\nu$ = 0.5–3.0 eV) at the spatial focusing point. The output from a dye laser (Lumonics HyperDYE-300) pumped with an excimer laser (Lumonics EXCIMER-600) was used in the range of $h\nu$ = 1.3–3.0 eV. The output from a dye laser (Spectra-Physics PDL-3) pumped with a Nd:YAG laser (Spectra-Physics GCR-18S) was frequency-shifted through a Raman shifter (Spectra-Physics RS-1) to generate near-infrared radiation from 0.9 to 1.6 eV. Difference-frequency mixing of the dye-laser output with the fundamental of the Nd:YAG laser in a $LiNbO_3$ crystal (Spectra-Physics WEX-2D) was employed in the range of $h\nu$ = 0.5–0.8 eV. The size of the $(C_6H_6)_n^+$ ions was selected by adjusting the delay time between the ion preparation and the laser irradiation. The resulting photofragment ions were mass-analyzed by the reflectron mass spectrometer and detected by a dual microchannel plate (Detector-1). Neutral photofragments were not retarded by the reflector and detected by another dual microchannel plate (Detector-2) situated behind the reflector.

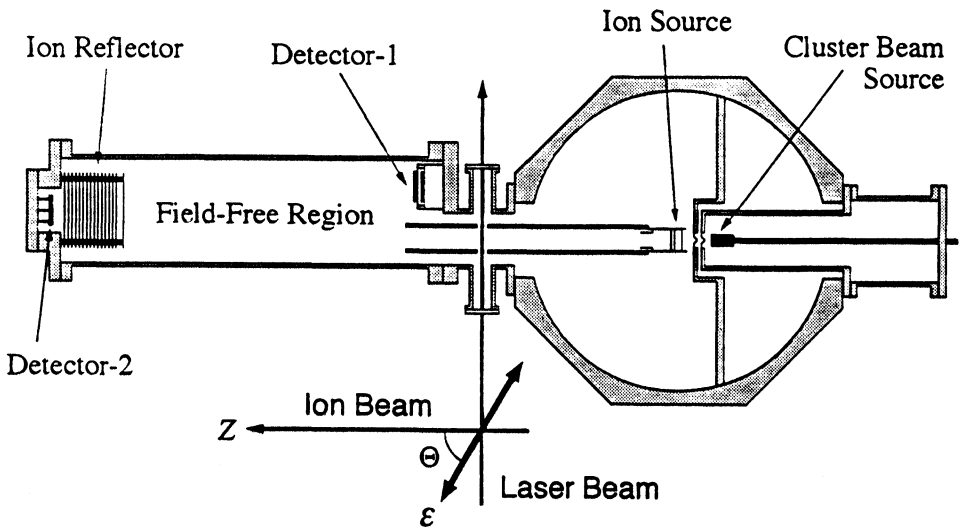

Figure 1 Schematic illustration of the cluster beam apparatus with the reflectron-type time-of-flight mass spectrometer. Photodissociation laser beam is introduced into the field-free region of the mass spectrometer. Detector-1 is used to detect photofragment ions, while Detector-2 is for the detection of neutral fragments. The angle between the laser polarization vector (ε) and the ion beam direction (Z) is denoted by Θ.

3. RESULTS AND DISCUSSION

3.1. Excited States of Benzene Cluster Ions

The photodissociation spectrum of $(C_6H_6)_2^+$ is displayed in Figure 2. The spectrum shows four different electronic transitions of $(C_6H_6)_2^+$ in the photon energy range from 0.9 to 3.0 eV.[10] Two broad maxima at $h\nu$ = 2.8 and 2.1 eV are assigned to local excitation (LE) bands. The two LE bands are due to electronic excitation ($\pi \leftarrow \pi$ transition and $\pi \leftarrow \sigma$ transition, respectively) of a monomer cation unit within $(C_6H_6)_2^+$. The upper states are bound with respect to the intermolecular coordinate. The most intense band at $h\nu$ = 1.35 eV is attributed to charge resonance (CR) band. The CR band arises from the transition between the bound ground state and its sister repulsive excited state. A relatively weak band at 1.07 eV is assigned to another CR band. The appearance of the two CR bands is explained on the basis of displaced sandwich structures for $(C_6H_6)_2^+$.[10] In the following sections, the four absorption bands at 2.8, 2.1, 1.35 and 1.07 eV are abbreviated to LE($\pi\pi$), LE($\sigma\pi$), CR1 and CR2 bands, respectively. The photodissociation spectrum of $(C_6H_6)_3^+$ in the

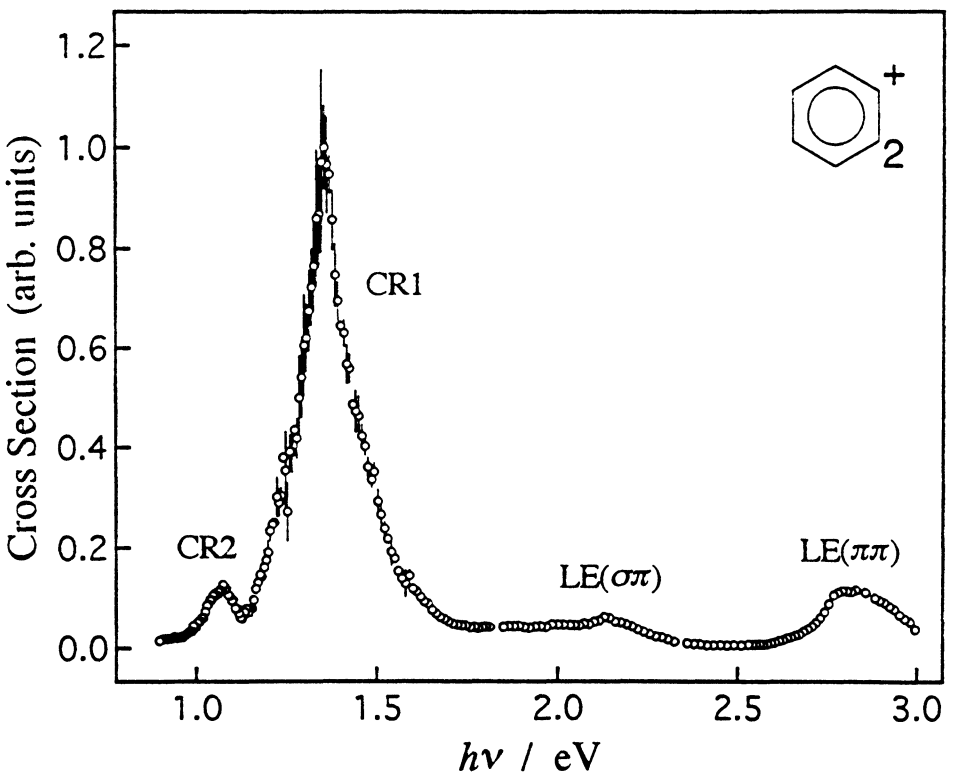

Figure 2 Photodissociation spectrum (plots of normalized yields of the fragment $C_6H_6^+$ ion against the photon energies) of $(C_6H_6)_2^+$. The four bands at $h\nu$ = 2.8, 2.1, 1.35 and 1.07 eV are referred to as LE($\pi\pi$), LE($\sigma\pi$), CR1 and CR2 bands, respectively, in the text.

CR band region exhibits similar features to that of $(C_6H_6)_2^+$: an intense maximum at 1.29 eV and a weak one at 1.02 eV.[24] The intense 1.29-eV band corresponds to the CR1 band of $(C_6H_6)_2^+$. The photodissociation cross sections at the 1.29-eV band are essentially equal to those of $(C_6H_6)_2^+$ at the CR1 band. These results suggest that the trimer band is due to the CR transition of the $(C_6H_6)_2^+$ subunit within $(C_6H_6)_3^+$.[9,24] Larger benzene cluster ions with $n > 3$ are also proposed to have a charge-localized structure,[25,26] $(C_6H_6)_2^+(C_6H_6)_{n-2}$, where $(C_6H_6)_2^+$ is the chromophoric unit for the CR absorption.[22] The $(C_6H_6)_2^+$ subunit and the rest of C_6H_6 molecules are referred to as "dimer core" and "surrounding molecules", respectively.

3.2. Size Distribution of Photofragment Ions

Excitation of $(C_6H_6)_n^+$ with photon energies below 3.66 eV causes loss of (N) neutral benzene molecules, but no fragmentation of benzene itself. The process can be expressed as

$$(C_6H_6)_n^+ + h\nu \rightarrow (C_6H_6)_{n-N}^+ + NC_6H_6. \quad (1)$$

Although no mass analysis of the neutral fragments is made here, they probably take the form of N monomers rather than a neutral cluster, i.e. $(C_6H_6)_N$. This point is discussed later in terms of the dissociation mechanisms of $(C_6H_6)_n^+$. Figure 3 shows the TOF mass spectra of the photofragment ions from $(C_6H_6)_6^+$ at four different photon energies. During the measurement, the photodissociation laser was introduced into the ion source (the acceleration region) in order to achieve large overlap between the parent ion bunch and the laser spot. The ion signals were accumulated with the dissociation laser on and then background signals due to metastable decay were accumulated with the laser off. The mass spectra of the photofragments were obtained by the subtraction of the laser-off spectra from the laser-on spectra. The negative peaks at the cluster size 5 are due to this subtraction and originated from the depletion of the metastable decay of $(C_6H_6)_6^+$ into $(C_6H_6)_5^+$ and C_6H_6 in the field-free region of the mass spectrometer. Since the parent ions were photoexcited in the acceleration region, slow fragmentation processes would lead to flight time asymmetry in the fragment ion signals.[27] The observation of symmetric peak shape for the photofragment ion signals implies a fast fragmentation process, occurring within the pulse width of the laser ($\leq$ 10 ns). The mass spectra show no indications of slower fragementation processes in the field-free region except the trimer ion peak on the spectrum obtained with $h\nu = 0.77$ eV. The dimer ion signal (marked with *) appeared on the same spectrum is probably due to 2-photon absorption process, although scrupulous care was taken for preventing multiphoton excitation. The following 2-step sequential absorption-fragmentation process is responsible for the formation of $(C_6H_6)_2^+$ in this case,

$$(C_6H_6)_6^+ \xrightarrow{h\nu} (C_6H_6)_4^+ + 2C_6H_6 \xrightarrow{h\nu} (C_6H_2)_2^+ + 4C_6H_6. \quad (2)$$

The ratio of the product ion intensities, $[(C_6H_6)_2^+]/[(C_6H_6)_4^+]$, increases with increasing laser power, supporting the above 2-photon mechanism. With increasing photon

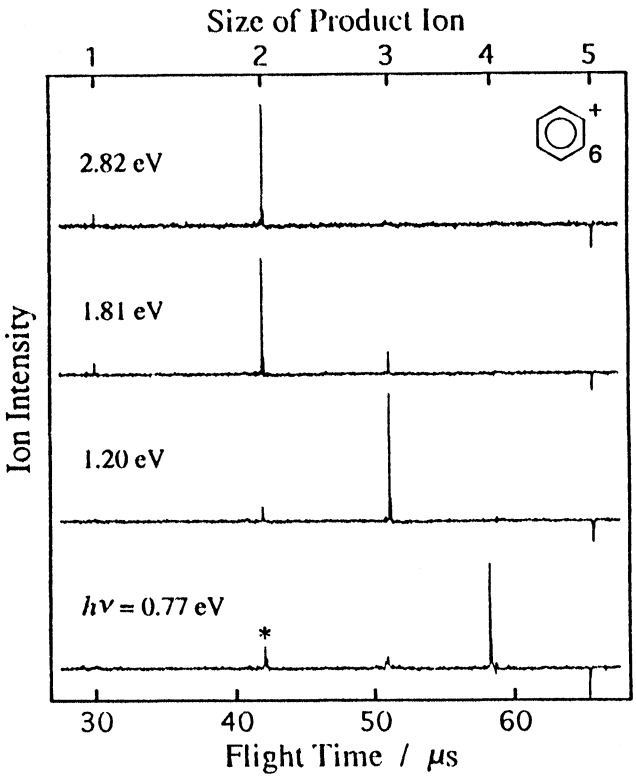

Figure 3 TOF mass spectra of the photofragment ions from $(C_6H_6)_6^+$ measured at four different photon energies in the range of $h\nu$ = 0.77 eV (bottom) to 2.82 eV (top). The dimer ion signal (marked by *) on the bottom spectrum is probably due to 2-photon absorption process (see text).

energy from $h\nu$ = 0.77 eV to 1.81 eV, the size of the dominant product ion becomes smaller from $(C_6H_6)_4^+$ to $(C_6H_6)_2^+$. Absorption of a photon in this energy range induces the CR transition of the dimer core. Further increase of $h\nu$ hardly changes the product distribution up to $h\nu$ = 2.82 eV.

The photofragmentation studies were conducted on the cluster ions from $(C_6H_6)_3^+$ to $(C_6H_6)_8^+$ at 21 different photon energies between 0.5 and 3.0 eV. The laser power was carefully controlled to ensure that 1-photon processes predominantly determine the size distributions of the fragment ions. The distributions are characterized by the parameter $\langle N \rangle$, the average number of C_6H_6 neutrals ejected following photoexcitation. This quantity is determined from the ratios of the observed photofragment ion intensities. Our attention is focused only on the fast fragmentation processes occurring within the laser pulse duration. Figure 4 illustrates the plots of $\langle N \rangle$ against $h\nu$ for $(C_6H_6)_n^+$ with n = 5–8. The $\langle N \rangle$ values increase linearly with increasing $h\nu$ in the low energy side of the CR band region. Each of the solid lines drawn through the experimental points is the result of a least-squares fit. Extrapolation of the lines for n = 6–8 to $h\nu$ = 0 eV results in $\langle N \rangle \approx 1$, showing that the parent ions originally

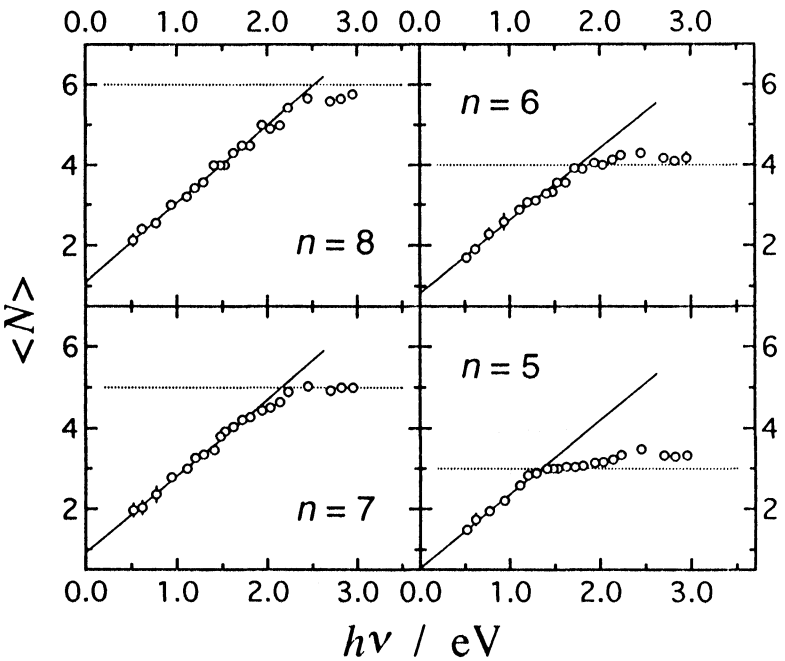

Figure 4 The average number of neutral C_6H_6 molecules ejected in the photodissociation of $(C_6H_6)_n^+$ (n = 5–8) as a function of photon energy. Each of the solid lines drawn through the experimental points (opened circles) in the CR band region is the result of a least-squares fit. The broken lines indicate the relation: $\langle N \rangle = n-2$ for each parent size.

have internal energies enough to release one surrounding molecule without being photoexcited. The broken lines in the figure indicate the relation: $\langle N \rangle = n-2$ for each parent size. When $h\nu$ amounts to the energy necessary for each parent ions to dissociate into $(C_6H_6)_2^+$, the $\langle N \rangle$ value stays constant at $n-2$ for a while. The dimer core can hold the deposited energy effectively due to its large binding energy (0.66 eV).[28] The behavior of $(C_6H_6)_7^+$ and $(C_6H_6)_8^+$ in the range of $h\nu$ = 2.1–3.0 eV may not be simply due to the stability of the dimer core, because bound upper states are involved in the photoexcitation. Figure 5 shows the plots of $\langle N \rangle$ against $h\nu$ for $(C_6H_6)_3^+$ and $(C_6H_6)_4^+$. For these small cluster ions, the dominant fragement ion is already $(C_6H_6)_2^+$ even at $h\nu \approx 0.7$ eV. Thus the conservation of particle number works on the value of $\langle N \rangle$.

3.3. Time-of-Flight Spectra of Neutral Fragments

The TOF spectra of the neutral fragments were measured to derive the translational energy distributions, including information on the angular distributions. As indicated in Figure 1, the photodissociation laser was introduced into the field-free region of the mass spectrometer. The polarization vector of the dissociation laser (ε) was rotated with respect to the ion beam direction (Z) by a double Fresnel rhomb retarder

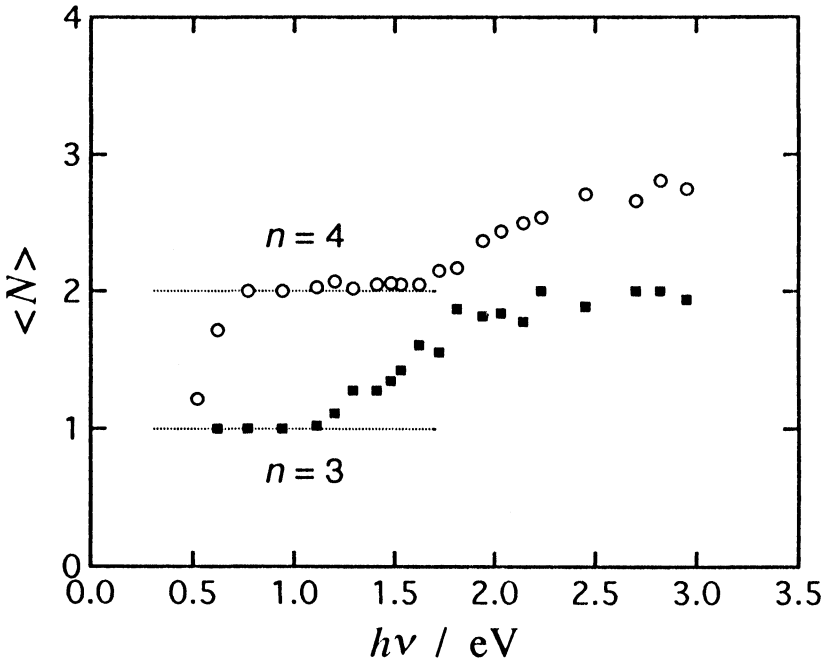

Figure 5 Plots of the average number of ejected molecules against photon energy for $(C_6H_6)_3^+$ (filled squares) and $(C_6H_6)_4^+$ (opened circles).

or a retardation plate. The angle between ε and Z is denoted by Θ hereafter. Measurement of the released translational energy was performed at the magic angle of $\Theta = 54.7°$ in order to eliminate any angular dependence. Typical results are exhibited in Figure 6 for the photodissociation of $(C_6H_6)_2^+$ and $(C_6H_6)_3^+$ at the LE($\pi\pi$) band ($h\nu$ = 2.81 eV). The figure represents the normalized distributions of arrival times onto Detector-2. The filled circles in the upper panel show the distribution of the parent $(C_6H_6)_2^+$ ion. The opened circles indicate the distribution of the neutral fragments recorded separately by reflecting all the ionic species away from the detector. The profile of the distribution reflects the projection of the fragment velocity along the Z axis. The width of the distribution of the fragments is obviously broader than that of the parent ion due to the additional translational energy released in the dissociation process. Analysis of these TOF spectra provides us quantitative data on the translational energy distribution of the neutral fragments.

For the photodissociation of the parent ion of mass M_p into the fragment ion of mass M_f and the neutral fragment of mass M_n, the average relative translational energy is given by[23,29]

$$\langle E_t \rangle \approx \left(\frac{U_0 W_t}{L} \right)^2 \frac{M_n}{2 M_p M_f}, \tag{3}$$

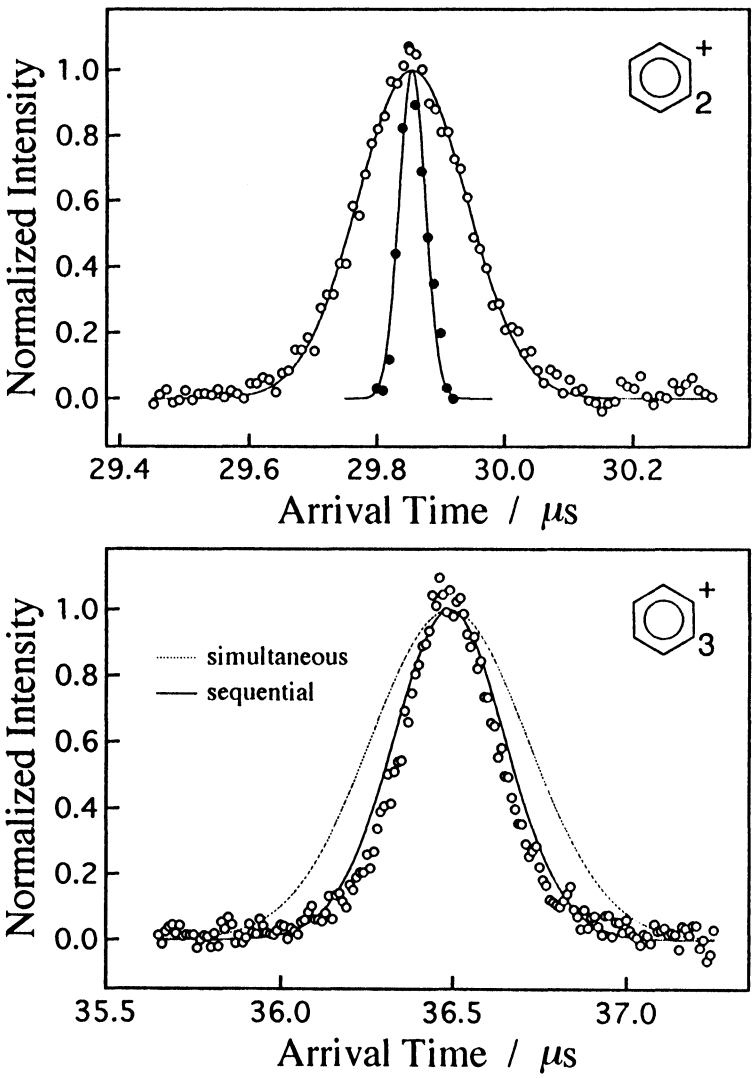

Figure 6 (upper) Normalized distributions of arrival times of the parent ion (filled circles) and the neutral fragment (opened circles) in the photodissociation of $(C_6H_6)_2^+$ at the LE($\pi\pi$) band ($h\nu$ = 2.81 eV). Each of the distributions is fitted with a Gauss function (solid curve) for the determination of $<E_t>$. (lower) Arrival-time distributions of the neutral fragment from $(C_6H_6)_3^+$ photodissociated at the LE($\pi\pi$) band ($h\nu$ = 2.81 eV). The opened circles stand for the experimental points, while the calculated distributions are indicated by the dotted and the solid curves according to the simultaneous and the sequential mechanisms, respectively.

where U_0 is the initial kinetic energy of the parent ion, L the drift length of the neutral fragment in the field-free region and W_t the measured broadening width of the arrival-time distribution of the neutral fragment. The broadening width can be obtained from the relation:

$$W_t^2 = W_n^2 - W_p^2, \tag{4}$$

where W_n is the width of the neutral fragment signal at 22% of the maximum and W_p is the width of the parent ion signal. Equation (4) is applicable only when both the parent and the fragment signals have Gaussian shapes.

Each of the arrival-time distributions in the upper panel of Figure 6 is fitted with a Gauss function (solid curve) for the determination of W_t. The following values are derived from the best fit: W_n = 298 ns and W_p = 80 ns. The average translational energy calculated from Equations (3) and (4) is $\langle E_t \rangle$ = 71 meV. This quantity can be obtained by an alternative method using the ion reflector and Detector-1, where the arrival-time distributions of the *fragment ions* are analyzed instead of the *neutral fragments*. Note that the arrival-time distributions of the ions at Detector-1 are strongly dependent on the reflector voltages, because the reflector has the ability to focus the energy spread of the ion bunch. The energy-focusing effect of the ion reflector should be carefully avoided in order to measure an accurate value of the broadening width.

3.4. Energy Partitionings

Prior to the investigations of the larger cluster ions, the photophysical properties of the bare $(C_6H_6)_2^+$ ion are examined in detail as the chromophoric subunit in the larger cluster ions. The average translational energy released in the photodissociation of $(C_6H_6)_2^+$ is plotted against the available energy in Figure 7. The experimental values for $\langle E_t \rangle$ are determined from the arrival-time distributions of either the fragment ion (opened circles) or the neutral fragment (filled circles). The available energy is given by

$$E_{av} = h\nu - E_0 + E_{int}, \tag{5}$$

where E_0 is the binding energy of $(C_6H_6)_2^+$ and E_{int} the initial internal energy before the photoexcitation. The binding energy of 0.66 ± 0.02 eV was determined by Ernstberger *et al.* from the measurement of the appearance potential of metastable monomer evaporation and the ionization potential of the dimer.[28] The value is consistent with an estimation of E_0 = 0.67 eV from the energy of the CR transition.[10] The initial internal energy is neglected in Figure 7, although the energy of $E_{int} \leq 0.1$ eV is estimated.[23] The neglect of E_{int} is not particularly crucial to the interpretation of the data.

For the photodissociation of $(C_6H_6)_2^+$ following the excitation at the LE($\pi\pi$) band ($h\nu$ = 2.81 eV), $\langle E_t \rangle$ is determined to be 69 ± 2 meV from the arrival-time distribution of the neutral fragment and 71 ± 4 meV from the fragment ion. Snodgrass *et al.* reported similar value of 70 ± 7 meV at $h\nu$ 2.71 eV.[7] The fraction of the available energy partitioned into the relative translational energy is only 3%. They concluded that this is because the upper state in the photoabsorption process is a bound state. The spectroscopic study by our group showed that the LE($\pi\pi$) state of $(C_6H_6)_2^+$ is indeed bound relative to $C_6H_6^+(\pi\pi) + C_6H_6(X)$,[8] where X stands for the ground electronic state. After the transition to the bound state, the available energy is ex-

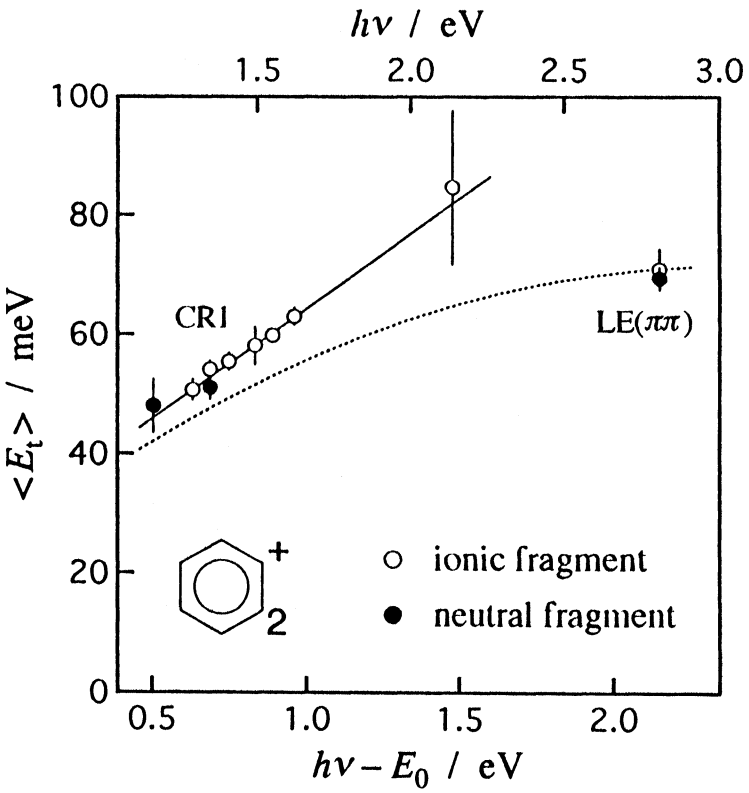

Figure 7 Plots of the average translational energy released in the photodissociation of $(C_6H_6)_2^+$ against available energy. The experimental values of $<E_t>$ are determined from the arrival-time distribution of either the fragment ion (opened circles) or the neutral fragment (filled circles). The solid line drawn through the data points in the CR1 band region is the result of a least-squares fit. The calculated values of $<E_t>$ by the statistical phase space theory are indicated by the dotted curve.

pected to be released in a statistical way with a small fraction partitioned into the translational motion. As indicated in Figure 7, the experimental value of $<E_t>$ agrees well with the prediction by the statistical phase space theory (dotted curve).[7,23]

For the photodissociation at the CR1 band, the measurement of $<E_t>$ is performed at 7 different photon energies between 1.17 eV and 1.62 eV. In this range, the average translational energy increases linearly with the available energy. The solid line drawn through the experimental data points is the result of a least-squares fit. The equation of the line is,

$$<E_t> = 0.037\ E_{av} + 0.027. \quad (6)$$

For a given increase in E_{av}, only ≈4% of that energy appears as the relative translational energy of the products. The CR transition of $(C_6H_6)_2^+$ corresponds to the bound-free transition of $(NO)_2^+$, $(N_2)_2^+$ and $(CO_2)_2^+$ observed in the visible region. However, the slope of $<E_t>$ plotted against E_{av} is much smaller than that of the dimer

ions of the small molecules, which is 0.51 for $(NO)_2^+$, 0.47 for $(N_2)_2^+$ and 0.31 for $(CO_2)_2^+$.[4–6] Although the experimental values of $\langle E_t \rangle$ do not coincide with the theoretical values by the statistical phase space calculation, the difference is not so large enough to be attributed to nonstatistical energy partitioning. The translational energy of the fragments is very small despite the expected nature of the repulsive excited state.

In atomic dimers, any excess energy (the available energy) should appear as the relative translational energy. In contrast, dimers of polyatomic molecules have a variety of dissociation mechanisms, because the available energy can flow into intramolecular modes, and energy randomization and dissociation compete.[30] Even if dissociation of such dimers proceeds on a repulsive potential surface, it is possible that a part of the available energy ends up as internal excitation of the fragments instead of the relative translation. Photodissociation is accompanied by vibrational excitation of the fragments because of the change in equilibrium geometry upon the electronic excitation and the dissociation.[31] The two benzene moieties of $(C_6H_6)_2^+$ in the ground state probably have an intermediate structure compared with those for separated C_6H_6 and $C_6H_6^+$, since the charge is shared with the two molecules.[9,10] The electronic excitation of $(C_6H_6)_2^+$ at the CR1 band produces a vibrationally excited pair of $C_6H_6^+ + C_6H_6$ because of large structural difference between the ground state $C_6H_6^+$ and C_6H_6.

Let us look briefly at the energetics for the photodissociation of the larger cluster ions, although we have not yet performed a systematic measurement on the released translational energy. The photon-energy dependence of the average number $\langle N \rangle$ allows us to deduce an evaporation energy per molecule from the cluster ion. As illustrated in Figure 4, the linear dependence of $\langle N \rangle$ on $h\nu$ in the CR band region implies that the evaporation energy is nearly constant over the cluster size from $n - \langle N \rangle$ to n for $(C_6H_6)_n^+$ (n = 5–8). The slope values of the lines demonstrate that the energy of 0.52–0.55 eV is required to remove one molecule. On the other hand, the bond dissociation energy, $E[(C_6H_6)_{n-1}^+ - C_6H_6]$, was determined to be 0.34 ± 0.02 and ≈0.3 eV for n = 3 and 4, respectively, from the equilibrium constants for the clustering reaction.[32] Krause *et al.* reported somewhat smaller values as follows: 0.27 ± 0.04 eV for n = 3, 0.13 ± 0.04 eV for n = 4 and ≤0.11 eV for n = 5.[33] The evaporation energies of $(C_6H_6)_n^+$ (n = 5–8) are much larger than the bond dissociation energies.

Conservation of energy requires the following relation:

$$E_{int} + h\nu = E'_{int} + E_t + E_d, \tag{7}$$

where E_{int} and E'_{int}, are the initial internal energy of the parent ion and the final internal energy of the products, respectively. E_t stands for the total translational energy of the products and E_d the sum of the dissociation energies for the broken bonds. In the photodissociation of $(C_6H_6)_2^+$ at the CR1 band, the released translational energy per molecule is 0.026 eV at $h\nu$ = 1.35 eV from Equation (6). One can take this value as an upper limit for the translational energy of a neutral molecule from the larger cluster ions, since the amount of E_t should be less significant for the larger clusters. In the photodissociation of $(C_6H_6)_4^+$ into $(C_6H_6)_2^+$ and $2C_6H_6$ at $h\nu$ = 1.35

eV, for example, the total translational energy is estimated to be $E_t \leq 0.07$ eV and the total binding energy is $E_d \leq 0.64$ eV from the bond dissociation energies. If the initial internal energy of the parent $(C_6H_6)_4^+$ is neglected, Equation (7) gives a lower limit for the internal energy of the products, $E'_{int} \geq 0.64$ eV. One can expect that the excess energy is distributed among the available bath modes, including possibly the intramolecular modes, prior to the fragmentation and that the products are vibrationally hot. Anyhow the energy at least ≈0.2 eV larger than the reported bond dissociation energy is required to remove one neutral molecule from the cluster ion following the CR band excitation.

3.5. Lifetime of Excited States

Effects of anisotropy in the angular distributions are most clearly seen when the arrival-time distribution measured at $\Theta = 0°$ is compared with that at $\Theta = 90°$. For the photodissociation of $(C_6H_6)_2^+$ at the LE($\pi\pi$) band ($h\nu = 2.81$ eV), no detectable difference is found among the arrival-time distributions recorded at $\Theta = 0°$, 54.7° and 90°, indicating that the product angular distribution is isotropic. For the photodissociation at the CR1 band, the widths of the arrival-time distributions of the fragment ion are always in the following order: $W_f(0°) > W_f(54.7°) > W_f(90°)$, but the difference between $W_f(0°)$ and $W_f(90°)$ is as small as 4–12%.

The probability that the products recoil at an angle θ with respect to the ion beam direction (Z) is given by[34]

$$P(\theta, \Theta) \propto \sin\theta\,[1 + \beta P_2(\cos\theta)\,P_2(\cos\Theta)], \tag{8}$$

where $P_2(\cos\theta)$ is the second degree Legendre polynomial in $\cos\theta$ and β is the asymmetry parameter which has values between +2 and −1 and characterizes the degree of anisotropy.[35] The isotropic distribution is represented by $\beta = 0$. A computer simulation of the arrival-time distributions is performed to extract quantitative knowledge of the anisotropy in the angular distributions. The simulation with $\beta = 0.2 \pm 0.1$ reasonably reproduces the experimental distributions for the photodissociation of $(C_6H_6)_2^+$ at the CR1 band.

The asymmetry parameter depends on the alignment of the transition dipole moment with the dissociation axis and on the time of dissociation.[36] The following values are reported for β in the visible photodissociation of the dimer ions of the small molecules: 1.3 for $(NO)_2^+$, 1.15–1.35 for $(N_2)_2^+$ and 1.0 for a high-energy component of $(CO_2)_2^+$.[4–6] These β-values indicate that the time of dissociation is less than a rotational period of the photoexcited parent ions. For the CR transition of $(C_6H_6)_2^+$, the transition dipole moment is expected to be predominantly parallel with the intermolecular axis. If this is the case, the small value of β should be mainly due to the rotational averaging. From the β-value of 0.2 ± 0.1, one can presume that the time of dissociation is comparable to or longer than a rotational period. The rotational period of $(C_6H_6)_2^+$ is estimated to be ≈1 ns with rotational quantum number $J = 1$, and it is ≈10 ps for $J = 10$. Such a time is quite long compared to the time scale expected for the excitation to the repulsive state.

3.6. Photodissociation Mechanism of $(C_6H_6)_2^+$

In the excitation at the LE($\pi\pi$) band, the photon is absorbed by a $C_6H_6^+$ unit within $(C_6H_6)_2^+$. The upper state is a bound state correlated to $C_6H_6^+(\pi\pi) + C_6H_6(X)$. The photon energy of 2.81 eV is not sufficient to reach the $C_6H_6^+(\pi\pi) + C_6H_6(X)$ or the $C_6H_6^+(\sigma\pi) + C_6H_6(X)$ dissociation asymptote. Thus both of the products, $C_6H_6^+$ and C_6H_6, should be formed in their ground electronic states. The $(C_6H_6)_2^+$ ions in the ($\pi\pi$) excited state probably undergo the internal conversion to vibrationally excited levels of the ground state. After the complete energy randomization among the available modes, the hot $(C_6H_6)_2^+(X)$ ions dissociate into $C_6H_6^+(X)$ and $C_6H_6(X)$ with a large amount of internal energy as a result of intermolecular vibrational predissociation.

A proposed photodissociation mechanism following the excitation at the CR1 band is as follows. The photon induces the transition of the dimer ion itself from the ground state to a dissociative excited state. The only accessible state with photon energies below 2.1 eV is the dissociative state correlated to $C_6H_6^+(X) + C_6H_6(X)$, because $C_6H_6^+$ has no low lying excited electronic states below the ($\sigma\pi$) state. An interpretation in terms of the transition to a low lying bound excited state is not applicable here. As $(C_6H_6)_2^+$ starts to move apart on the dissociative potential surface, the breaking intermolecular bond is dynamically coupled to the intramolecular vibrational modes of the fragments. Since the motion of the atoms during the dissociation is not simply one of extension of the intermolecular distance, a simple picture based on the one-dimensional potential energy curve is not adequate to describe the photodissociation of $(C_6H_6)_2^+$ at least in the case of the CR band excitation. This is probably because $(C_6H_6)_2^+$ has 66 vibrational modes and mode mixing among the intermolecular and the intramolecular vibrational modes could be highly important. Energy flow between these modes in the excited $(C_6H_6)_2^+$ could be so fast that the behavior becomes almost statistically controlled, in contrast to the dynamical control in the dimer ions of the small molecules.

3.7. Photodissociation Mechanism of $(C_6H_6)_3^+$

Following the excitation of $(C_6H_6)_3^+$ at the LE($\pi\pi$) band, only $C_6H_6^+$ is observed as the product ion. This is clear from Figure 5, which shows that the number of the ejected molecules is just 2 at around $h\nu = 2.8$ eV. Three fragments ($C_6H_6^+$ and $2C_6H_6$) are most likely produced, since the formation of $(C_6H_6)_2$ is improbable because of the small binding energy (0.07 ± 0.01 eV)[28] of $(C_6H_6)_2$. Baer *et al.* considered the problem of energy partitioning in a dissociation process which leads to the formation of three fragments.[37,38] Their model requires that there is sufficient interaction between the fragments and that the energy partitioning can be described by a statistical theory. Two of the cases cited by Baer *et al.* are the simultaneous (three-body) dissociation:

$$(C_6H_6)_3^+ \xrightarrow{h\nu} C_6H_6^+ + C_6H_6 + C_6H_6, \tag{9}$$

and the sequential (two-step) dissociation:

$$(C_6H_6)_3^+ \xrightarrow{h\nu} (C_6H_6)_2^+ + C_6H_6[I] \rightarrow C_6H_6^+ + C_6H_6[II] + C_6H_6[I]. \quad (10)$$

In the latter case, the transient $(C_6H_6)_2^+$ is formed by instantaneous ejection of the neutral $C_6H_6[I]$. Dissociation of the transient dimer follows, yielding the neutral $C_6H_6[II]$ and $C_6H_6^+$. One can deal with the energy partitioning in the photodissociation of $(C_6H_6)_3^+$ at the LE($\pi\pi$) band by a statistical theory, in analogy with the case of $(C_6H_6)_2^+$ as mentioned in section 3.4. By using expressions based on the equipartition theorem,[37,38] average translational energies of the fragments are calculated for the two cases (9) and (10). The results are converted into arrival-time distributions and displayed in the lower panel of Figure 6 by the dotted and the solid curves for the simultaneous and the sequential mechanisms, respectively. The calculated arrival-time distribution according to the sequential mechanism (solid curve) is in better agreement with the experimental distribution. Similar two-step mechanism was suggested for the formation of Ar^+ from Ar_3^+ by Woodward *et al.*[39] and the formation of CO_2^+ from $(CO_2)_3^+$ by Kim *et al.*,[40] after photoexcitation in the visible region.

For the photodissociation following the CR band excitation, the complete randomization of the available energy may not be achieved as in the case of $(C_6H_6)_2^+$. As one can notice from Figure 5, only the formation of $(C_6H_6)_2^+$ is possible (i.e. $\langle N \rangle = 1$) below $h\nu \approx 1.0$ eV. At photon energies between 1.0 and 2.0 eV, both $C_6H_6^+$ and $(C_6H_6)_2^+$ are observed as the product ions and the branching ratio is dependent on $h\nu$. The $\langle N \rangle$ value increases smoothly from 1 to 2 with increasing $h\nu$. This behavior is in contrast to the case of $(NO)_3^+$ reported by Jarrold *et al.*[41] They observed both NO^+ and $(NO)_2^+$ as the photofragment ions. The fraction of $(NO)_2^+$ is essentially independent of the photon energy in the range of $h\nu = 1.87$–2.66 eV. They suggested that the photodissociation occurs via the direct transition to a repulsive surface. The product channels are therefore expected to be determined dynamically. On the other hand, the behavior of $(C_6H_6)_3^+$ seems to be qualitatively consistent with a quasiequilibrium theory for unimolecular reactions.[42,43]

3.8. Photofragmentation Mechanism of $(C_6H_6)_n^+$ ($n \geq 4$)

There are two limiting cases of photofragmentation mechanisms. One limit is *direct dissociation*, in which dynamical effects dominate the fragmentation with the amount of energy deposited in cluster ions playing only a secondary role. This mechanism usually involves the simultaneous dissociation of the energized cluster ions into multiple fragments. The other limit is *evaporation* which is governed principally by the total energy. The evaporative mechanism is analogous to the quasiequilibrium theory for unimolecular dissociation and is based on the concept of energy randomization in the cluster ions.

The photon-energy dependence of the average number of the ejected molecules gives an insight into the type of fragmentation process (sequential monomer ejection vs fission). The two processes have been described for different cluster systems. Geusic *et al.* reported that the neutral C_3 loss is the dominant channel in the

photofragmentation of C_n^+.[11] This fission process is supported by the fact that the photofragmentation pattern is *independent of the photon energy*. The photofragmentation of cluster ions of main-group elements (Si, Ge, Sb, Te, Bi and so forth) is also proposed to be dominated by similar fission processes.[12–15] On the other hand, the average number of the atoms lost in the photofragmentation of K_n^+ was reported to be *proportional to the photon energy*.[16] Such a behavior was also observed in the photofragmentation of $(CO_2)_n^+$, $(CO_2)_n^-$ and Ar_n^+ by Lineberger and co-workers.[17–19] They concluded that the photofragmentation processes proceed via the ejection of neutral monomers rather than a neutral cluster.

The formation of a neutral cluster through fission process is not necessarily the result of direct dissociation. The dominance of the C_3 loss channel in the photofragmentation of C_n^+ is considered to reflect the fact that it is the lowest energy pathway.[11] Geusic *et al.* mentioned that the photofragmentation would not be a direct process but would involve a transition to a bound excited state followed by internal conversion to vibrationally excited levels of the ground state. Fragmentation then occurs statistically on the ground state potential surface to give preferentially the lowest energy products. In general, experimental data to date on the fragmentation of large cluster ions seem to be consistent with the statistical mechanism.[16–19] Product channels are therefore expected to be determined thermodynamically rather than dynamically.

Recently, a combination of the direct and the evaporative mechanisms was found in the photofragmentation of Ar_n^+ by Smith *et al.*[44] and by Nagata and Kondow.[45] For Ar_n^+ with $7 \leq n \leq 12$, the translational energy distribution of the neutral fragments shows a bimodal behavior. The high-energy component arises from the direct dissociation of a trimer ion core, which is followed by evaporation of the surrounding atoms leading to production of the low-energy fragments. In the larger cluster ions with $n \geq 14$, production of the high-energy fragments is suppressed. The photofragmentation proceeds as a unimolecular decay of the vibrationally hot cluster ions.[45]

In the photofragmentation of $(C_6H_6)_n^+$ with n = 3–8, no sudden change of the fragmentation patterns is observed as we vary the photon energy from 0.5 to 3.0 eV. Beck and Hecht studied the photofragmentation of $(C_6H_6)_n^+$ with n = 7–15 in the photon-energy range of $h\nu$ = 1.38–1.78 eV.[22] They observed a smooth transition in the fragmentation pattern from loss of 3 neutral molecules to loss of 4 with increasing $h\nu$, which is consistent with our data. As shown in Figure 4 for $(C_6H_6)_n^+$ with n = 5–8, the average number of the neutral molecules ejected following photoexcitation increases linearly with increasing $h\nu$ until $(C_6H_6)_2^+$ is reached as the product ion. The linear dependence of $\langle N \rangle$ on $h\nu$ allows us to deduce that the fragmentation occurs predominantly via the sequential loss of C_6H_6 monomers. If the loss of neutral clusters were a major decay pathway, the dependence of $\langle N \rangle$ on $h\nu$ would be stepwise rather than linear (smooth). At a given photon energy, the $\langle N \rangle$ values are essentially independent of the parent cluster size, suggesting that the photofragmentation is controlled by the amount of energy deposited in the cluster ions. It should be noted that the behaviors of such small benzene cluster ions (n = 5–8) are similar to those of *large* Ar_n^+ cluster ions ($n \geq 40$).[19] From these observations, we can expect that the evaporative process governs the photofragmentation of the benzene cluster ions as small as $(C_6H_6)_5^+$.

The following mechanism can be described for the photofragmentation of $(C_6H_6)_n^+$, part of which has already been proposed by Beck and Hecht.[22] At photon energies of less than ≈2 eV, the dimer core in $(C_6H_6)_n^+$ behaves as a chromophore. The photoabsorption arises from the CR transition of the dimer core and it is promoted to a dissociative excited state. In contrast to the case of Ar_n^+ ($7 \leq n \leq 12$), however, direct dissociation of the photoexcited dimer core seems to be unlikely, because the photophysical behavior is almost statistically controlled even in the case of the bare $(C_6H_6)_2^+$. As demonstrated for the bare $(C_6H_6)_2^+$, the time of dissociation of the dimer core would be quite long compared to the time scale expected for the direct dissociation. We speculate therefore that the instantaneous ejection of a moiety from the dimer core does not take place at the first stage of the fragmentation. Instead, as the dimer core begins to separate on the dissociative potential surface, the intermolecular mode along the dissociation coordinate is coupled to the van der Waals modes of the ground state. The initial electronic energy stored in the dimer core is rapidly converted into the vibrational energy of the cluster ion. It is reasonable to expect that the energy is randomized throughout the available modes of the ground state, since the energy flow among these modes would be much faster than the separation of the dimer core. The vibrationally hot cluster ion then decays by evaporating the surrounding molecules. The sequential evaporation of the neutral monomers continues until the temperature of the cluster ion becomes low enough to retain the most weakly bound molecule. The photofragmentation process can be regarded as a unimolecular decay of the vibrationally hot cluster ion regardless of the promotion of the chromophoric dimer core to the repulsive excited state.

Direct observation of the vibrationial excitation in the products will be helpful to confirm the above mechanism. Number densities of photofragments from size-selected cluster ions, however, are generally too low to allow conventional methods to be applied. Determination of the translational energy distribution of the fragments is an alternative method, as it provided useful information on the photofragmentation mechanism of Ar_n^+.[44,45] Detailed measurement is in progress to record the time-of-flight spectra of both the ionic and neutral fragments in the photodissociation of $(C_6H_6)_n^+$ as a function of photon energy.

4. CONCLUSIONS

The upper state of the CR transition of $(C_6H_6)_2^+$ is repulsive, while the LE($\pi\pi$) state is bound with respect to the intermolecular coordinate. The photoexcitation to the bound LE($\pi\pi$) state results in the statistical energy disposal. Following the excitation to a repulsive state, on the other hand, the excess energy is usually released in a dynamical way. The most remarkable finding from the present study is that regardless of the photoexcitation to the repulsive CR state, the released translational energy is very small and the angular distribution of the fragments is almost isotropic. From these observations we can expect that the energy flow among the available modes in the photoexcited $(C_6H_6)_2^+$ is so fast that the photophysical behavior becomes almost statistically controlled, in contrast to the dynamically controlled behavior of the dimer

ions of the small molecules such as $(NO)_2^+$, $(N_2)_2^+$ and $(CO_2)_2^+$.

The larger $(C_6H_6)_n^+$ ions with $n \geq 3$ are proposed to have a charge-localized structure, $(C_6H_6)_2^+(C_6H_6)_{n-2}$, where $(C_6H_6)_2^+$ is the chromophoric unit for the CR absorption. For the photofragmentation of $(C_6H_6)_n^+$ (n = 5–8) in the CR band region, the average number of the ejected molecules increases linearly with increasing $h\nu$ until $(C_6H_6)_2^+$ is reached as the product ion. At a given photon energy, however, the number is essentially independent of the parent cluster size. These observations suggest that the photofragmentation proceeds via the sequential evaporation of neutral monomers rather than the direct ejection of a neutral cluster. Despite the promotion of the chromophoric dimer core to the repulsive excited state, the subsequent fragmentation process can be regarded as a unimolecular decay of the vibrationally hot cluster ion.

Acknowledgements

This work was supported in part by a Grant-in-Aid for New Program "Intelligent Molecular Systems with Controlled Functionality" (06NP0301) and general research programs (04403002 and 05740364) from the Ministry of Education, Science and Culture of Japan.

References

1. *Ion and Cluster Ion Spectroscopy and Structure*, edited by J. P. Maier (Elsevier, Amsterdam, 1989).
2. *Cluster Ions*, edited by C. Y. Ng, T. Baer and I. Powis (Wiley, Chichester, 1993).
3. E. J. Bieske and J. P. Maier. *Chem. Rev.*, **93**, 2603 (1993).
4. M. F. Jarrold, A. J. Illies and M. T. Bowers. *J. Chem. Phys.*, **79**, 6086 (1983).
5. M. F. Jarrold, A. J. Illies and M. T. Bowers, *J. Chem. Phys.*, **81**, 214 (1984).
6. A. J. Illies, M. F. Jarrold, W. Wagner-Redeker and M. T. Bowers. *J. Phys. Chem.*, **88**, 5204 (1984).
7. J. T. Snodgrass, R. C. Dunbar and M. T. Bowers. *J. Phys. Chem.*, **94**, 3648 (1990).
8. K. Ohashi and N. Nishi. *J. Chem. Phys.*, **95**, 4002 (1991).
9. K. Ohashi and N. Nishi. *J. Phys. Chem.*, **96**, 2931 (1992).
10. K. Ohashi, Y. Nakai, T. Shibata and N. Nishi. *Laser Chem.*, **14**, 3 (1994).
11. M. E. Geusic, M. F. Jarrold, T. J. McIlrath, R. R. Freeman and W. L. Brown *J. Chem. Phys.*, **86**, 3862 (1987).
12. L. A. Bloomfield, R. R. Freeman and W. L. Brown. *Phys. Rev. Lett.*, **54**, 2246 (1985).
13. Y. Liu, Q.-L. Zhang, F. K. Tittel, R. F. Curl and R. E. Smalley. *J. Chem. Phys.*, **85**, 7434 (1986).
14. M. E. Geusic, R. R. Freeman and M. A. Duncan. *J. Chem. Phys.*, **88**, 163 (1988).
15. K. F. Willey, P. Y. Cheng, T. G. Taylor, M. B. Bishop and M. A. Duncan. *J. Phys. Chem.*, **94**, 1544 (1990).
16. C. Bréchignac, Ph. Cahuzac and J.-Ph. Roux. *J. Chem. Phys.*, **88**, 3022 (1988).
17. M. L. Alexander, M. A. Johnson and W. C. Lineberger, *J. Chem. Phys.*, **82**, 5288 (1985).
18. M. L. Alexander, M. A. Johnson, N. E. Levinger and W. C. Lineberger. *Phys. Rev. Lett.*, **57**, 976 (1986).
19. N. E. Levinger, D. Ray, M. L. Alexander and W. C. Lineberger. *J. Chem. Phys.*, **89**, 5654 (1988).
20. C. E. Klots. *Z. Phys. D*, **5**, 83 (1987).
21. C. E. Klots. *J. Phys. Chem.*, **92**, 5864 (1988).
22. S. M. Beck and J. H. Hecht. *J. Chem. Phys.*, **96**, 1975 (1992).
23. K. Ohashi and N. Nishi. *J. Chem. Phys.*, **98**, 390 (1993).
24. T. Shibata, K. Ohashi, Y. Nakai and N. Nishi. to be published.
25. K. E. Schriver, A. J. Paguia, M. Y. Hahn, E. C. Honea, A. M. Camarena and R. L. Whetten. *J. Phys. Chem.*, **91**, 3131 (1987).
26. K. Ohashi, Y. Nakai and N. Nishi. *At. Collision Res. Jpn. Prog. Rep.*, **18**, 84 (1992).

27. H. Kühlewind, H. J. Neusser and E. W. Schlag. *Int. J. Mass Spectrom. Ion Phys.*, **51**, 255 (1983).
28. B. Ernstberger, H. Krause, A. Kiermeier and H. J. Neusser. *J. Chem. Phys.*, **92**, 5285 (1990).
29. S. Wei, W. B. Tzeng and A. W. Castleman, Jr. *J. Chem. Phys.*, **92**, 332 (1990).
30. R. N. Dixon. *Acc. Chem. Res.*, **24**, 16 (1991).
31. R. C. Mitchell and J. P. Simons. *Discuss. Faraday Soc.*, **44**, 208 (1967).
32. K. Hiraoka, S. Fujimaki, K. Aruga and S. Yamabe. *J. Chem. Phys.*, **95**, 8413 (1991).
33. H. Krause, B. Ernstberger and H. J. Neusser. *Chem. Phys. Lett.*, **184**, 411 (1991).
34. M. F. Jarrold, A. J. Illies and M. T. Bowers, *J. Chem. Phys.*, **82**, 1832 (1985).
35. R. N. Zare. *Mol. Photochem.*, **4**, 1 (1972).
36. S. Yang and R. Bersohn. *J. Chem. Phys.*, **61**, 4400 (1974).
37. T. Baer, A. E. DePristo and J. J Hermans. *J. Chem. Phys.*, **76**, 5917 (1982).
38. T. E. Carney and T. Baer. *J. Chem. Phys.*, **76**, 5968 (1982).
39. C. A. Woodward, J. E. Upham, A. J. Stace and J. N. Murrell. *J. Chem. Phys.*, **91**, 7612 (1989).
40. H.-S. Kim, M. F. Jarrold and M. T. Bowers, *J. Chem. Phys.*, **84**, 4882 (1986).
41. M. F. Jarrold, A. J. Illies and M. T. Bowers. *J. Chem. Phys.*, **81**, 222 (1984).
42. R. G. Cooks, J. H. Beynon, R. M. Caprioli and G. R. Lester. *Metastable Ions* (Elsevier, Amsterdam, 1973).
43. P. C. Engelking. *J. Chem. Phys.*, **85**, 3103 (1986).
44. J. A. Smith, N. G. Gotts, J. F. Winkel, R. Hallett, C. A. Woodward, A. J. Stace and B. J. Whitaker. *J. Chem. Phys.*, **97**, 397 (1992).
45. T. Nagata and T. Kondow. *J. Chem. Phys.*, **98**, 290 (1993).